

# Phases of asymmetric nuclear matter with broken space symmetries

H. Mütter and A. Sedrakian

*Institut für Theoretische Physik, Universität Tübingen, D-72076 Tübingen, Germany*

(November 11, 2018)

## Abstract

Isoscalar Cooper pairing in isospin asymmetric nuclear matter occurs between states populating two distinct Fermi surfaces, each for neutrons and protons. The transition from a BCS-like to the normal (unpaired) state, as the isospin asymmetry is increased, is intervened by superconducting phases which spontaneously break translational and rotational symmetries. One possibility is the formation of a condensate with a periodic crystallinelike structure where Cooper pairs carry net momentum (the nuclear Larkin-Ovchinnikov-Fulde-Ferrell-phase). Alternatively, perturbations of the Fermi surfaces away from spherical symmetry allow for minima in the condensate free energy which correspond to a states with quadrupole deformations of Fermi surfaces and zero momentum of the Cooper pairs. In a combined treatment of these phases we show that, although the Cooper pairing with finite momentum might arise as a local minimum, the lowest energy state features are deformed Fermi surfaces and Cooper pairs with vanishing total momentum.

arXiv:nucl-th/0209061v3 26 Apr 2004

## I. INTRODUCTION

The pairing properties of nuclear systems - finite nuclei and the bulk nuclear matter - play an important role in the physical manifestations of these systems. In most cases of interest the pairing occurs at finite isospin asymmetry. For example, charge neutral bulk nuclear matter with an admixture of leptons in  $\beta$  equilibrium implies proton abundancies at about 40% in supernova matter and 10% in neutron star matter. The dominant partial-wave channel for the pairing depends on the density, temperature, and the isospin asymmetry in general. For large enough asymmetries the matter is paired in the isospin triplet channels - the  $^1S_0$  channel at low densities [1–11] and  $^3P_2$ - $^3F_2$  or  $^1D_2$  channels at high densities [12–20]. For weakly asymmetric systems the isospin singlet attractive  $^3S_1$ - $^3D_1$  [22–27] and  $^3D_2$  channels [28,29] dominate the pairing interaction at low and high densities, respectively. In bulk nuclear matter of compact stars the asymmetries are most likely too large to support isospin singlet pairing. However the dilute nuclear matter in supernovas and the low-density tails of the exotic nuclei can support  $^3S_1$ - $^3D_1$ -channel pairing, since in general the isospin asymmetry is less effective in destroying the pair correlations in dilute matter [25].

The mechanism of the suppression of the BCS pairing of the kind found in asymmetric nuclear matter was initially studied in metallic superconductors in a spin-polarizing magnetic field [30–33]. Since a homogenous magnetic field is screened beyond the London penetration depth in the bulk of a superconductor, in real materials the electron spin polarization is induced by low-density paramagnetic impurities, which interact with an electron by spin nonconserving forces. The effect of collision induced polarization is commonly modeled by an average polarizing field which implies an asymmetry in the populations of spin-up and -down quasiparticles. The resulting electron Pauli paramagnetism suppresses the  $S$ -wave pairing when the Fermi surfaces of the electrons with spin-up and -down are apart on a scale of the order of the energy gap in the quasiparticle spectrum. A close analogy to the ordinary superconductors can be seen in the effect of the large  $B$  fields in the neutron stars on the  $S$ -wave pairing of neutrons. Our general discussion below also applies to the pairing in spin-polarized neutron matter in the  $^1S_0$  channel, although the numerical computations are carried out for the isoscalar pairing in asymmetric matter.

The understanding of the isospin singlet pairing as a function of the isospin asymmetry requires an extension of the standard BCS theory to describe phases with spontaneously broken space symmetries. Larkin and Ovchinnikov [34] and Fulde-Ferrell [35] (LOFF) argued, in the context of metallic superconductors, that a transition from the BCS paired to the normal state occurs via a phase where the Cooper pairs carry a finite total momentum. The isospin polarization in nuclear matter with pairing in the  $^3S_1$ - $^3D_1$  channel leads to a nuclear LOFF phase for a range of isospin asymmetries [36,37]. Unlike the metallic superconductors where the ratio of the pairing gap to the average chemical potential is of the order  $10^{-3}$ , the nuclear LOFF phase emerges in the strong coupling regime, where this ratio is of the order 0.1. The spatially periodic structure of the nuclear LOFF phase corresponding to oscillations of the condensate wave function are on the scales of the order of several fm. Note that, independent of the detailed structure of the lattice, the LOFF phase breaks *both* the translational and rotational invariance of the original BCS state. The formation of the LOFF phase is a robust feature of the fermionic systems with broken time-reversal symmetry and has been studied in detail in the flavor asymmetric high-density QCD (crystalline

color superconductivity) [38–45].

The evolution of the condensate from the BCS to paired states with broken space symmetries, as the isospin asymmetry is increased, can take a different path if we give up the assumption that the intrinsically homogeneous matter features spherical Fermi surfaces [46]. As shown in ref. [46], for quadrupole deformed Fermi surfaces (DFS) the BCS condensate evolves to a state with spontaneously broken rotational symmetry [in group theory terms the  $O(3)$  symmetry breaks down to  $O(2)$ ]. Such a state is still axially symmetric and, unlike the LOFF phase, preserves the translational symmetry. We shall refer to the superconducting state with deformed Fermi surfaces as the DFS phase with the understanding that the expansion describing the deformation of Fermi surfaces is truncated at quadrupole order (the higher order terms in the multiple expansion have not been studied so far).

Why do the phases with broken space symmetries dominate the BCS state? The BCS quasiparticle spectrum (for homogeneous systems) is isotropic; when the polarizing field drives apart the Fermi surfaces of fermions with spin/isospin up and down the phase space overlap is lost, hence the pairing is suppressed. The finite momentum of the Cooper pairs of the LOFF phase implies an anisotropic quasiparticle spectrum; the magnitude of the anisotropy is controlled by the value of the net momentum of the pairs which is treated as a parameter. This new degree of freedom, which can be viewed as an additional variational parameter for the minimization of the ground state of the system, (partially) overcomes the phase-space loss caused by the departure of the Fermi surfaces from the perfectly overlapping configuration. In effect the gain in the pairing energy through increase of the pairing field dominates the increase of the kinetic energy. To motivate the DFS phase, note that formally the LOFF spectrum can be viewed as a dipole ( $\propto P_1(x)$ ) perturbation of the spherically symmetrical BCS spectrum, where  $P_l(x)$  are the Legendre polynomials, and  $x$  is the cosine of the angle between the particle momentum and the total momentum of the Cooper pair. The DFS phase assumes an expansion of the quasiparticle spectrum up to the next-to-leading order, quadrupole ( $\propto P_2(x)$ ) deformation; it also assumed that the total momentum of the Cooper pairs is zero, i.e., there are quadrupole deformations only. Although the perturbations from the spherical symmetry cost kinetic energy, they are compensated by the gain in the potential energy. For a range of asymmetries the DFS phase becomes the ground state of the paired system [46].

The purpose of the present paper is a combined treatment of the LOFF and the DFS phases in bulk isospin asymmetric nuclear matter within the same model as that in Refs. [36,46]. The model assumes a pairing force given by a phase-shift equivalent (i.e., realistic) interaction and nonrenormalized quasiparticle spectrum. The effect of the mean field in the Brueckner-Hartree-Fock approximation is to reduce the range of isospin asymmetries where the pairing exists [24]. We shall follow the strategy of disentangling the effects of the mean field from the pairing since already at the level of approximations of Refs. [36,46] the LOFF and DFS phases show a complicated behavior. The renormalization of the quasiparticle spectrum for the pairing interaction is a problem of its own which has not been solved to date. Issues such as the consistency between the vertex and propagator renormalization and fulfillment of the spectral sum rules, etc. need further attention.

In Section 2 we derive the BCS equations, which include the effects of the finite momentum of the Cooper pairs and Fermi surface deformations, within the finite-temperature real-time Green's functions formalism. The numerical solutions of these equations are pre-

sented in Section 3, where we discuss the phase diagram of the combined LOFF and DFS phases and their properties at finite temperatures. Section 4 contains a summary of the results and an outlook.

## II. FORMALISM

The starting point of the model is the Hamiltonian of fermions interacting via two-body forces:

$$H = \frac{1}{2m} \sum_{\alpha} \int d^3r \vec{\nabla} \psi^{\dagger}(\vec{r}, t, \alpha) \vec{\nabla} \psi(\vec{r}, t, \alpha) + \frac{1}{2} \sum_{\alpha\beta} \int d^3r d^3r' \psi^{\dagger}(\vec{r}, t, \alpha) \psi^{\dagger}(\vec{r}', t, \beta) V(\vec{r}, t, \alpha; \vec{r}', t, \beta) \psi(\vec{r}, t, \beta) \psi(\vec{r}, t, \alpha), \quad (1)$$

where  $\psi(\vec{r}, t, \alpha)$  are second quantized operators in the Heisenberg representation,  $V_{\alpha,\beta}(\vec{r} - \vec{r}')\delta(t - t')$  is the space and time local bare interaction, and  $\alpha, \beta$  stand for discrete quantum numbers (spin, isospin, etc.). We choose to formulate the finite-temperature pairing theory in terms of nonequilibrium real-time Green's functions. The single-particle propagator in this formalism is combined in a  $2 \times 2$  matrix,

$$\underline{\hat{G}}(x_1, x_2) = \begin{pmatrix} \hat{G}^c(x_1, x_2) & \hat{G}^<(x_1, x_2) \\ \hat{G}^>(x_1, x_2) & \hat{G}^a(x_1, x_2) \end{pmatrix} = \begin{pmatrix} -i\langle T \hat{\psi}(x_1) \hat{\psi}^{\dagger}(x_2) \rangle & i\langle \hat{\psi}^{\dagger}(x_2) \hat{\psi}(x_1) \rangle \\ -i\langle \hat{\psi}(x_1) \hat{\psi}^{\dagger}(x_2) \rangle & -i\langle \tilde{T} \hat{\psi}(x_1) \hat{\psi}^{\dagger}(x_2) \rangle \end{pmatrix}, \quad (2)$$

where  $x \equiv (\vec{r}, t, \alpha)$ , and the averaging is over an arbitrary nonequilibrium state of the system;  $T$  and  $\tilde{T}$  are chronological and antichronological time ordering operators for the Nambu spinors

$$\hat{\psi}^{\dagger} = [\psi^{\dagger}(x)\psi(x)] \quad \hat{\psi} = \begin{bmatrix} \psi(x) \\ \psi^{\dagger}(x) \end{bmatrix}. \quad (3)$$

The Nambu spinors span the particle-hole space and satisfy the fermionic equal-time anti-commutation relations

$$\{\hat{\psi}_{\alpha}(\vec{x}, t), \hat{\psi}_{\beta}^{\dagger}(\vec{x}', t)\} = \delta_{\alpha\beta} \delta^3(\vec{x} - \vec{x}'), \quad \{\hat{\psi}_{\alpha}(\vec{x}, t), \hat{\psi}_{\beta}(\vec{x}', t)\} = 0, \quad \{\hat{\psi}_{\alpha}(\vec{x}, t)^{\dagger}, \hat{\psi}_{\beta}^{\dagger}(\vec{x}', t)\} = 0.$$

Starting from the equations of motion for the Heisenberg operators and the Hamiltonian (1) the Martin-Schwinger hierarchy can be constructed for a matrix Green's function involving an arbitrary number of field operators. For our purposes it is sufficient to truncate the hierarchy at the  $n = 1$  level. The equation of motion of a one-particle Green's function is then given by the time-dependent Dyson equation

$$\hat{\underline{G}}_{(0)}^{-1}(x_1) \otimes \hat{\underline{G}}(x_1, x_2) = \sigma_z \delta(x_1 - x_2) - \hat{\underline{V}}(x_1, x_6; x_5, x_4) \otimes \hat{\underline{G}}(x_5, x_4, x_2, x_6^+), \quad (4)$$

where the subscript (0) refers to the free propagator,  $\otimes$  stands for summation/integration over the repeated discrete/continuous variables,  $\sigma_i$  are the components of the vector of the Pauli matrices, and the superscript  $+$  means an infinitesimal increment in the time argument.

The hierarchy at a given level can be decoupled (formally) by introducing the self-energy matrix:

$$\hat{\underline{G}}_{(0)}^{-1}(x_1) \otimes \hat{\underline{G}}(x_1, x_2) = \sigma_z \delta(x_1 - x_2) + \hat{\underline{\Sigma}}(x_1, x_3) \otimes \hat{\underline{G}}(x_3, x_2), \quad (5)$$

which is defined as

$$\hat{\underline{\Sigma}}(x_1, x_2) = -\hat{\underline{V}}(x_1, x_6; x_5, x_4) \otimes \hat{\underline{G}}(x_5, x_4, x_7, x_6^+) \hat{\underline{G}}^{-1}(x_7, x_2). \quad (6)$$

The first of these equations defines the quasiparticle spectrum of the superconducting state, the second, the self-energies, e.g., the gap function. To close the set of exact equations we need to specify the approximation to the two-particle Green's function. The BCS theory follows in the Hartree approximation, where the two-particle Green's function is approximated by a product of single-particle Green's functions. Note that the anomalous contributions of the type  $\langle \psi(x_1) \psi(x_2) \rangle$  and  $\langle \psi^\dagger(x_1) \psi^\dagger(x_2) \rangle$  are automatically built in in the Hartree approximation. This can be verified from the explicit form of the propagator in Eq. (2), when the spinors (3) are substituted. Each element of the  $2 \times 2$  matrix (2) is in turn a  $2 \times 2$  matrix in the particle-hole space:

$$\hat{G}_{12}^j = \begin{pmatrix} G^j(x_1, x_2) & F^j(x_1, x_2) \\ F^{\dagger j}(x_1, x_2) & \bar{G}^j(x_1, x_2) \end{pmatrix}, \quad (7)$$

where  $j \equiv c, a, >, <$ . The matrix form of the self-energies in the particle-hole space is analogous to that of the propagators:

$$\hat{\underline{\Sigma}}(x_1, x_2) = \begin{pmatrix} \hat{\Sigma}^c(x_1, x_2) & \hat{\Sigma}^<(x_1, x_2) \\ \hat{\Sigma}^>(x_1, x_2) & \hat{\Sigma}^a(x_1, x_2) \end{pmatrix}, \quad \hat{\Sigma}^j(x_1, x_2) \equiv \begin{pmatrix} \Sigma^j(x_1, x_2) & \Delta^j(x_1, x_2) \\ \Delta^{\dagger j}(x_1, x_2) & \bar{\Sigma}^j(x_1, x_2) \end{pmatrix}, \quad (8)$$

where the off-diagonal elements of the  $\Sigma^j(x_1, x_2)$  matrix correspond to the pairing amplitude. Note that the inverse free-particle propagator is diagonal in the particle-hole,  $j$  and spin/isospin spaces:

$$G_{(0)\alpha\beta}^{-1} = (i\partial_t + \nabla^2/2m_\alpha - \mu_\alpha) \delta_{\alpha\beta}. \quad (9)$$

The Dyson Eq. (5) is a  $16 \times 16$  matrix equation in general if we include the spin and isospin. The size of the matrix to be diagonalized can be reduced in several successive steps. Here we note that in the time-independent stationary limit the number of the propagators can be reduced by applying the unitary transformation  $U = (1 + i\sigma_y)/\sqrt{2}$  to Eqs. (5) and (6), in the  $j$  space, and introducing the retarded/advanced propagators by the relations

$$G^{R,A}(x_1, x_2) = G^c(x_1, x_2) - G^{<, >}(x_1, x_2) = G^{>, <}(x_1, x_2) - G^a(x_1, x_2). \quad (10)$$

Further reductions will be carried out in the next section. The Dyson equation, e.g., for the retarded propagator is invariant under the rotation in the  $j$  space affected by the transformation above, i.e.,

$$\hat{G}^R(x_1, x_2) = \hat{G}_{(0)}^R(x_1, x_2) + \hat{G}_{(0)}^R(x_1, x_2) \otimes \hat{\Sigma}^R(x_1, x_3) \otimes \hat{G}^R(x_3, x_2); \quad (11)$$

the retarded self-energies are related to the matrix components in the  $j$  space by relations analogous to Eq. (10). The integral Eq. (11) for the retarded propagators can be solved without specifying the approximation to (and hence the form of) the self-energies, in the quasiclassical approximation.

## A. Quasiparticle spectrum

When the characteristic length scales of the spatial variations of the macroscopic condensate are much larger than the inverse of the momenta involved in the problem  $\sim p_F$ , where  $p_F$  is the Fermi momentum, the two-point correlation functions can be approximated by their quasiclassical counterparts. Going over to the center of mass  $X = (x_1 + x_2)/2$  and relative  $\xi = x_1 - x_2$  coordinates in the two-point functions and carrying a Fourier transform with respect to the relative coordinates we arrive at the mixed representation for these functions, e.g.,

$$\hat{G}^<(p, X) = \int e^{ip\xi} \hat{G}^<\left(X + \frac{\xi}{2}, X - \frac{\xi}{2}\right) d^4\xi, \quad (12)$$

where  $p \equiv (\omega, \mathbf{p})$  are the relative frequency and momentum, and  $X \equiv (\mathbf{R}, T)$ . Since the variations of the propagators and self-energies are slow on the scales of the order of  $\mathbf{R}$ , keeping the leading order terms in the gradient expansion is accurate to order  $\sim \mathcal{O}(p_F R)$ . The quasiclassical counterpart of the Dyson Eq. (11) is

$$\sum_{\gamma} \begin{pmatrix} \omega - \epsilon_{\alpha\gamma}^+ & -\Delta_{\alpha\gamma}^R(\omega, \mathbf{p}) \\ -\Delta_{\alpha\gamma}^{\dagger R}(\omega, \mathbf{p}) & \omega + \epsilon_{\alpha\gamma}^- \end{pmatrix} \begin{pmatrix} G_{\gamma\beta}^R(\omega, \mathbf{p}) & F_{\gamma\beta}^R(\omega, \mathbf{p}) \\ F_{\gamma\beta}^{\dagger R}(\omega, \mathbf{p}) & \bar{G}_{\gamma\beta}^R(\omega, \mathbf{p}) \end{pmatrix} = \delta_{\alpha\beta} \hat{\mathbf{1}}, \quad (13)$$

where

$$\epsilon_{\alpha\beta}^{\pm} = [(\mathbf{P}/2 \pm \mathbf{p})^2 / 2m_{\alpha} - \mu_{\alpha}] \delta_{\alpha\beta} \pm \Sigma_{\alpha\beta}^{R,(+)}(\omega, \mathbf{P}/2 \pm \mathbf{p}) - \Sigma_{\alpha\beta}^{R,(-)}(\omega, \mathbf{P}/2 \pm \mathbf{p}),$$

and  $\hat{\mathbf{1}}$  is a unit matrix in the particle-hole space. Here we have defined the symmetric and antisymmetric combinations of the particle/hole retarded self-energies

$$\Sigma_{\alpha\beta}^{R,(+)}(\omega, \mathbf{p}) \equiv \frac{1}{2} \left[ \Sigma_{\alpha\beta}^R(\omega, \mathbf{p}) + \bar{\Sigma}_{\alpha\beta}^R(\omega, \mathbf{p}) \right], \quad (14)$$

$$\Sigma_{\alpha\beta}^{R,(-)}(\omega, \mathbf{p}) \equiv \frac{1}{2} \left[ \Sigma_{\alpha\beta}^R(\omega, \mathbf{p}) - \bar{\Sigma}_{\alpha\beta}^R(\omega, \mathbf{p}) \right]. \quad (15)$$

The dependence on the center-of-mass time is dropped in the above expressions in the stationary limit. The retarded self-energies now can be expanded in Legendre polynomials:

$$\Sigma_{\alpha\beta}^{R,(+/-)}(\omega, \mathbf{p}) = \sum_{l=0}^{\infty} \Sigma_{\alpha\beta,2l}^{R,(+/-)}(\omega, p) P_l(\text{Cos } \theta), \quad (16)$$

where  $\theta$  is the angle between the vectors  $\mathbf{p}$  and  $\mathbf{P}$ . In practice the expansion will be truncated at order  $l = 2$ ; the  $l = 0$  term renormalizes the chemical potential, as discussed below. For translationally invariant interactions the odd terms do not contribute in the expansion (16); the interactions are assumed to be timelocal. For translationally noninvariant interactions the effect of the  $l = 1$  term would be a renormalization of the dipole deformation in the spectrum due to the kinetic energy terms. It can be included in the renormalization of the particle mass entering the anisotropic contribution to the kinetic energy, although it would not contribute to the net isotropic increase of the kinetic energy due to the finite momentum. Since the total momentum is treated as a variational parameter in the problem, the effect

of the self-energy renormalization at  $l = 1$  can be accounted for by a simple rescaling of this parameter; therefore we anticipate that the  $l = 1$  terms would not change the results below.

For spin and isospin conserving forces the normal Green's functions and self-energies are diagonal in the spin and isospin spaces. It is sufficient to consider the anomalous propagators, e.g., in the isospin space, since the resulting spin structure, for  $S$ -wave interactions, is uniquely determined for each isospin combination. If we restrict ourselves to the neutron-proton pairing in the  ${}^3S_1$ - ${}^3D_1$  channel, which is justified when  $\Delta_{nn}, \Delta_{pp} \ll \Delta_{np}$  (subscripts  $n$  and  $p$  refer to protons and neutrons) then  $\Delta_{\alpha\beta} = \sigma_x \Delta$ . The spectrum, in this case, takes the form

$$\omega_{\pm} = E_A \pm \sqrt{E_S^2 + |\Delta|^2}, \quad (17)$$

where the symmetric and asymmetric parts of the spectrum (which are even and odd with respect to the time-reversal symmetry) are defined as

$$E_S = \frac{1}{2}(\epsilon_+ + \epsilon_-), \quad E_A = \frac{1}{2}(\epsilon_+ - \epsilon_-). \quad (18)$$

The eigenvalues (17) are valid for an arbitrary approximation to the self-energies. Further, we shall approximate the symmetric and antisymmetric parts of the spectra using (i) the quasiparticle and (ii) the momentum-independent self-energy shift approximations. The first approximation implies

$$\Sigma_{n/p}^{R,(-/+)}(\mathbf{p}, \omega) \simeq \text{Re}\Sigma_{n/p}^{R,(-/+)}(\mathbf{p}, \epsilon_p) \simeq \text{Re}\Sigma_{n/p}^{R,(-/+)}(\mathbf{p}, \epsilon_p)\Big|_{p_F} + \frac{\partial}{\partial \mathbf{p}} \text{Re}\Sigma_{n/p}^{R,(-/+)}(\mathbf{p}, \epsilon_p)\Big|_{p_F} (p - p_F); \quad (19)$$

the second approximation keeps the leading order (constant) term in the expansion (19). Within these approximations we obtain

$$E_S = \frac{P^2}{8m} + \frac{p^2}{2m} - \mu - (\mu\epsilon + \delta\epsilon\delta\mu) \cos^2 \theta, \quad (20)$$

$$E_A = \frac{Pp}{2m} \cos \theta - \delta\mu + (\mu\delta\epsilon + \epsilon\delta\mu) \cos^2 \theta, \quad (21)$$

where we defined the average chemical potential and the conformal deformation

$$\mu = \frac{1}{2} [\mu_n + \mu_p] - \frac{1}{2} [\Omega_n^-(p_F) + \Omega_p^-(p_F)], \quad (22)$$

$$\epsilon = \frac{3}{4\mu} \text{Re} [\Sigma_{n,2}^{R(-)}(p_F) + \Sigma_{p,2}^{R(-)}(p_F)], \quad (23)$$

as the  $l = 0$  and  $l = 2$  contributions from the isospin symmetric part of the quasiparticle spectra; similarly the relative chemical potential and the relative deformation are defined as the  $l = 0$  and  $l = 2$  contributions from the isospin antisymmetric part of the quasiparticle spectra:

$$\delta\mu = \frac{1}{2} [\mu_n - \mu_p] - \frac{1}{2} [\Omega_n^+(p_F) - \Omega_p^+(p_F)], \quad (24)$$

$$\delta\epsilon = \frac{3}{4\mu} \text{Re} [\Sigma_{n,2}^{R(+)}(p_F) - \Sigma_{p,2}^{R(+)}(p_F)], \quad (25)$$

where we used the abbreviation

$$\Omega_{n/p}^{-/+}(p_F) = \text{Re} \left[ \Sigma_{n/p,0}^{R(-/+)}(p_F) - \frac{1}{2} \Sigma_{n/p,2}^{R(-/+)}(p_F) \right]. \quad (26)$$

The self-energies on the right-hand side of Eqs. (22)-(25) are functionals of the pairing field, i.e., they are nonzero even in the case where all the interactions apart from the pairing interaction are switched off. They depend on the quasiparticle momentum via the momentum dependence of the gap function; if the latter is approximated by its value at the Fermi momentum the self-energies become constants. The values of the average and relative chemical potentials  $\mu$  and  $\delta\mu$  can be adjusted to reproduce the particle density at a given temperature and isospin asymmetry. The conformal and relative deformations  $\epsilon$  and  $\delta\epsilon$  along with the finite momentum of the pairs  $P$  are treated as variational parameters to be determined from the ground state of the superconducting system.

The solution of the Dyson Eq. (13) for the propagators can be written in terms of the eigenvalues as

$$G_{n/p}^R(\omega, \mathbf{p}) = \frac{u_p^2}{\omega - \omega_{+/-} + i\eta} + \frac{v_p^2}{\omega - \omega_{-/+} + i\eta}, \quad (27)$$

$$F^R(\omega, \mathbf{p}) = u_p v_p \left( \frac{1}{\omega - \omega_+ + i\eta} - \frac{1}{\omega - \omega_- + i\eta} \right), \quad (28)$$

where the Bogolyubov amplitudes are

$$u_p^2 = \frac{1}{2} + \frac{E_S}{2\sqrt{E_S^2 + |\Delta|^2}}, \quad v_p^2 = \frac{1}{2} - \frac{E_S}{2\sqrt{E_S^2 + |\Delta|^2}}. \quad (29)$$

The remainder Green's functions can be reconstructed using the spectral representation of the retarded Green's functions

$$G_{n/p}^R(\omega, \mathbf{p}) = \int_{-\infty}^{\infty} d\omega' \frac{A_{n/p}(\omega', \mathbf{p})}{\omega - \omega' + i\eta}, \quad (30)$$

$$F^R(\omega, \mathbf{p}) = \int_{-\infty}^{\infty} d\omega' \frac{B(\omega', \mathbf{p})}{\omega - \omega' + i\eta}, \quad (31)$$

where  $A_{n/p}(\omega, \mathbf{p})$  and  $B(\omega, \mathbf{p})$  are the spectral functions. The Kadanoff-Baym ansatz [47] provides the link between the the retarded components and the remainder Green's functions in the  $j$  space. We have

$$G_{n/p}^{>,<}(\omega, \mathbf{p}) = A_{n/p}(\omega, \mathbf{p}) f^{>,<}(\omega), \quad (32)$$

$$F^{>,<}(\omega, \mathbf{p}) = B(\omega, \mathbf{p}) f^{>,<}(\omega), \quad (33)$$

where, in equilibrium, the Wigner distribution functions of the Kadanoff-Baym ansatz [47] reduce to the Fermi distribution function  $f^<(\omega) = [\exp(\beta\omega) + 1]^{-1}$  and  $f^>(\omega) = [1 - f^<(\omega)]$ ; here  $\beta$  is the inverse temperature. Note that the relations above are exact in the equilibrium limit. The causal and acausal Green's functions are then obtained from the relations (10).



## B. The gap equation

The BCS gap equation follows from the Hartree approximation for the two-particle Green's function in Eq. (4):

$$\hat{\underline{G}}(x_1, x_2; x_3, x_4) = \hat{\underline{G}}(x_1, x_2) \otimes \hat{\underline{G}}(x_3, x_4), \quad (34)$$

which implies, according to Eq. (6),

$$\hat{\underline{\Sigma}}(x_1, x_2) = -\hat{\underline{V}}(x_1, x_3; x_2, x_4) \otimes \hat{\underline{G}}(x_4, x_3^+). \quad (35)$$

Upon applying the quasiclassical approximation to the above equation in the case of time local interaction, we obtain the retarded (off diagonal in the particle-hole space) self-energy

$$\Delta^R(\mathbf{p}, \mathbf{P}) = \int \frac{d^3 p' d\omega'}{(2\pi)^4} V(\mathbf{p}, \mathbf{p}') F^<(\omega', \mathbf{p}', \mathbf{P}), \quad (36)$$

or using the relation  $F^<(\omega, \mathbf{p}) = -2\text{Im}F(\omega, \mathbf{p})f(\omega)$ , which follows from Eqs. (31) and (33),

$$\Delta^R(\mathbf{p}, \mathbf{P}) = - \int \frac{d^3 p' d\omega'}{(2\pi)^4} V(\mathbf{p}, \mathbf{p}') \text{Im}F^R(\omega', \mathbf{p}', \mathbf{P}) f^<(\omega'). \quad (37)$$

Further progress requires partial-wave decomposition of the interaction, which can be performed after angle averaging the remainder functions on the right-hand side of Eq. (37). The result of this procedure is

$$\Delta_l^R(p, P) = - \sum_{l'} \int \frac{dpp^2}{(2\pi)^2} V_{ll'}(p, p') \frac{\Delta_{l'}^R(p', P)}{2\sqrt{\epsilon_S^2 + \Delta(p', P)^2}} \langle [f^<(\omega_+) - f^<(\omega_-)] \rangle, \quad (38)$$

where  $\langle \dots \rangle$  denotes the average over the angle between the relative and total momenta and  $\Delta(p, P)^2 \equiv \Delta_0(p, P)^2 + \Delta_2(p, P)^2$  is the angle averaged gap. Here the pairing interaction is approximated by the bare neutron-proton interaction  $V(\mathbf{p}, \mathbf{p}')$  in the  ${}^3S_1$ - ${}^3D_1$  channel. As discussed above the average and relative chemical potentials can be fixed by adjusting the pairing field to reproduce the matter density  $\rho = \rho_n + \rho_p$  and the isospin asymmetry  $\alpha = (\rho_n - \rho_p)/\rho$ . The total momentum, the relative and conformal deformations, are treated as variational parameters to be determined from the ground state energy of the system. The corresponding expression for partial densities of protons and neutrons is provided by the relation

$$\rho_{n/p} = \int \frac{d^4 p}{(2\pi)^4} G_{n/p}^<(\omega, \mathbf{p}), \quad (39)$$

or, using Eqs. (30) and (32),

$$\rho_{n/p} = -2 \sum_{\sigma} \int \frac{d^4 p}{(2\pi)^4} \text{Im}G_{n/p}(\omega, \mathbf{p}) f(\omega) = \sum_{\sigma} \int \frac{d^3 p}{(2\pi)^3} \{u_p^2 f^<(\omega_{\pm}) + v_p^2 f^<(\omega_{\mp})\}, \quad (40)$$

where  $\sigma$  stands for quasiparticle spin and the second relation follows in the quasiparticle approximation.

### C. Thermodynamics

The phase diagram of the paired state at fixed finite temperature and density can be obtained from the free energy in the mean field approximation. The free energy is given by the thermodynamic relation

$$\mathcal{F}|_{\rho,\beta} = \mathcal{U} - \beta^{-1}S. \quad (41)$$

where  $\mathcal{U}$  is the internal energy and  $S$  is the entropy. A thermodynamically stable paired state minimizes the difference of the free energies of the superconducting and normal states,  $\delta\mathcal{F} \equiv \mathcal{F}_S - \mathcal{F}_N$ . The mean field entropy of the superfluid state is

$$S_S = -2k_B \sum \left\{ f^<(\omega_+) \ln f^<(\omega_+) + f^>(\omega_+) \ln f^>(\omega_+) + f^<(\omega_-) \ln f^<(\omega_-) + f^>(\omega_-) \ln f^>(\omega_-) \right\}, \quad (42)$$

where  $k_B$  is the Boltzmann constant and the sum is over the momentum states in the quasiparticle approximation. The corresponding expression for the entropy of the normal state  $S_N$  is obtained by taking the limit  $\Delta \rightarrow 0$  in Eq. (42). The internal energy of the superconducting state in the mean field approximation is

$$\mathcal{U}_S = 2 \int \frac{d^3p}{(2\pi)^3} \left\{ \left[ \epsilon^+ n_n(p) + \epsilon^- n_p(p) \right] + \sum_{l'} \frac{d^3p'}{(2\pi)^3} V_{ll'}(p, p') \nu_l(p) \nu_{l'}(p') \right\}, \quad (43)$$

where the normal and superconducting occupation probabilities are defined as

$$n_{n/p}(p) \equiv u_p^2 f^<(\omega_{\pm}) + v_p^2 f^<(\omega_{\mp}), \quad \nu(p) \equiv u_p v_p [f^<(\omega_+) - f^<(\omega_-)]. \quad (44)$$

The first term in Eq. (43) includes the kinetic energy of quasiparticles which is a functional of the pairing gap. In the normal state it reduces to the kinetic energy of noninteracting quasiparticles. The second term describes the BCS mean-field interaction among the particles in the condensate and vanishes in the normal state.

## III. RESULTS

The nuclear LOFF and DFS phases were studied numerically using the Paris nucleon-nucleon interaction. Our results did not depend on this choice of the interaction, since there are no significant deviations in the scattering phase shifts in the  ${}^3S_1 - {}^3D_1$  channel among various realistic potentials and these reproduce the properties of the deuteron at the same level of accuracy. The net density of the matter was fixed at the empirical saturation density of the nuclear matter  $\rho_s = 0.17 \text{ fm}^{-3}$ . At this density the typical energies of the nucleons are below the threshold laboratory energy  $E_{LAB} = 220 \text{ MeV}$  at which the interaction in the  ${}^3S_1 - {}^3D_1$  channel becomes repulsive. Lower densities could provide a more realistic (from the physical point of view) setting, however, they have the disadvantage that the effects of the Bose-Einstein condensation of deuterons may start to play a role [25]. The computations were carried out for several fixed values of the density asymmetry  $\alpha$  that are above the critical values at which the nuclear LOFF and DFS phases set in (see Refs. [36,46]). The qualitative behavior of quantities of interest is generic for different values of  $\alpha$ , therefore, we shall show the results for a fixed value  $\alpha = 0.35$  at which the LOFF and DFS phases (separately) dominate the ordinary BCS state.

## FIGURES

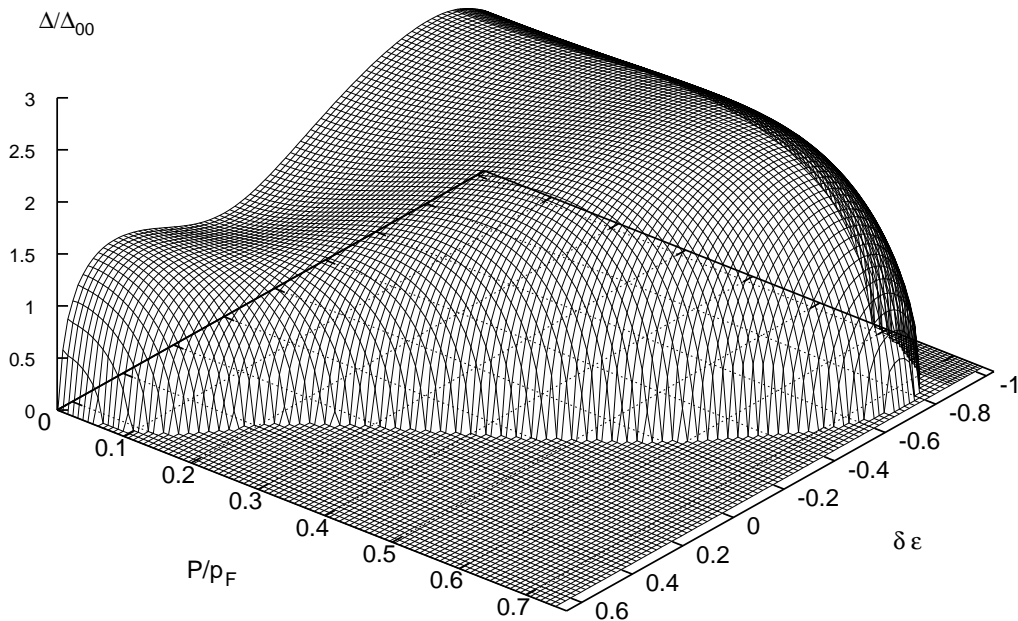


FIG. 1. The pairing gap as a function of a Cooper pair momentum  $P$  in units of Fermi momentum and the relative deformation parameter  $\delta\epsilon$ . The density asymmetry is fixed at the value  $\alpha = 0.35$ . The temperature and the density are  $T = 3$  MeV and  $\rho_s = 0.17$  fm $^{-3}$ , respectively. The gap is normalized to its value  $\Delta_{00}$  in the asymmetric BCS state.

The results of the combined treatment of the LOFF and DFS phases will be presented in two steps: in the next section we fix temperature and vary simultaneously the net momentum of the pairs  $P$  (LOFF phase) and the relative deformation  $\delta\epsilon$  (DFS phase). In the subsequent section we study the temperature dependence of these phases at either constant  $P$  or  $\delta\epsilon$ .

### A. LOFF versus DFS

Figure 1 shows the pairing gap as a function of the total momentum of Cooper pairs  $P$  and the relative deformation  $\delta\epsilon$  for vanishing conformal deformation ( $\epsilon = 0$ ). The temperature is fixed at the value  $T = 3$  MeV. The ratios of the temperature over the Fermi energy and the pairing gap in the symmetric state are 0.1 and 0.4 respectively, i.e., they correspond to the low-temperature regime. The gap is normalized to its value  $\Delta_{00} \equiv \Delta(P = 0, \delta\epsilon = 0)$  in the rotationally/translationally invariant state at  $\alpha = 0.35$ . Although  $\alpha \equiv (\rho_n - \rho_p)/(\rho_n + \rho_p)$  changes in the interval  $[-1; 1]$  in general, the symmetry of the equations with respect to

the indices labeling the species reduces the range of  $\alpha$  to  $[0; 1]$ . The relative deformation obviously is not bounded and can assume both positive and negative values. Positive values of  $\delta\epsilon$  imply an oblate deformation for the Fermi surface of neutrons and a prolate deformation for the Fermi surface of protons. The behavior of the pairing gap can be understood by examining the effect of the symmetric and antisymmetric parts of the quasiparticle spectrum on the gap Eq. (38). The antisymmetric part  $E_A$  appears only in the Fermi distribution functions. If  $E_A = 0$  one recovers the BCS limit, where the Fermi distribution functions become identical, i.e., the Fermi surfaces perfectly coincide. In this limit the phase-space overlap between the paired states is maximal. Consider the effect of a finite  $E_A$  when  $P = 0 = \delta\epsilon$ . It increases/decreases the energies of the isospin up/down particles; the shift in the Fermi-levels of the isospin up/down particles samples different momentum regions of the phase-space in the kernel of the gap equation. This blocking effect or phase-space decoherence in the pair states in turn reduces the magnitude of the gap. In particular this allows for pairs with small  $E_A$ . Switching on a finite  $P$  and/or  $\delta\epsilon > 0$  acts to restore partially the phase space coherence of the isospin up/down states when  $\delta\mu \geq \max\{Pp/2m, \mu\delta\epsilon\}$  [see Eq. (21)]. Therefore, the magnitude of the gap increases in this case, i.e. the phase-space overlap of the Fermi surfaces is (partially) restored. Increasing  $P$  and/or  $\delta\epsilon > 0$  further acts in a manner similar to pure energy shift  $\delta\mu$  - the decoherence increases and the pairing is eventually destroyed. This picture is seen in Fig. 1 in the region  $\delta\epsilon > 0$ . Small perturbations in  $P$  and  $\delta\epsilon$  from the asymmetric BCS state ( $P = 0 = \delta\epsilon$  but  $\delta\mu \neq 0$ ) increase the pairing gap. For large perturbation in either  $P$  or  $\delta\epsilon > 0$  the gap vanishes as the decoherence increases. The combined effect of the finite momentum and the quadrupole deformations is seen in the minimum plateau in the region of small  $P$  and  $\delta\epsilon$ , followed by a maximum in the gap with increasing  $P$  and/or  $\delta\epsilon$ , and a rapid falloff beyond the maximum. The behavior of the gap in the limits of pure LOFF and DFS phases is the same as the one found in the previous work [36,46].

In the case of  $\delta\epsilon < 0$  the  $\mu\delta\epsilon$  term in Eq. (21) combines with the chemical potential shift  $\delta\mu$ . To satisfy a given particle number asymmetry there are now two parameters (while there was only one,  $\delta\mu$ , for positive  $\delta\epsilon$ ). As a result with increasing deformation and hence  $\mu\delta\epsilon$  (the changes in  $\mu$  are insignificant) the density asymmetry can be maintained at a cost of smaller  $\delta\mu$  which tends to zero and eventually changes the sign ( $\mu_p > \mu_n$ ) at  $\delta\epsilon \sim -1$ . This marks the “turnover” in the gap equation which eventually vanishes for  $\delta\epsilon > -1$ . We shall see that the regions of the negative values of the deformation parameter are physically not relevant, since these states have larger kinetic energies. As in the case of positive  $\delta\epsilon$  the effect of finite momentum is to suppress the pairing for a large deformation; the combined phase increases the pairing only for small perturbations from the asymmetric BCS state in the vicinity of the “minimum plateau” ( $\delta\epsilon \rightarrow 0, P \rightarrow 0$ ). The symmetric part of the quasiparticle spectrum (20) controls the location of the maximum (corresponding to  $E_S = 0$ ) and the width of the kernel in Eq. (38) in the momentum space through its contribution to the denominator of the gap equation. A positive contribution to the average chemical potential effectively decreases the density of states (which can be easily seen analytically in the zero temperature and weak coupling limits), and therefore, the gap function.

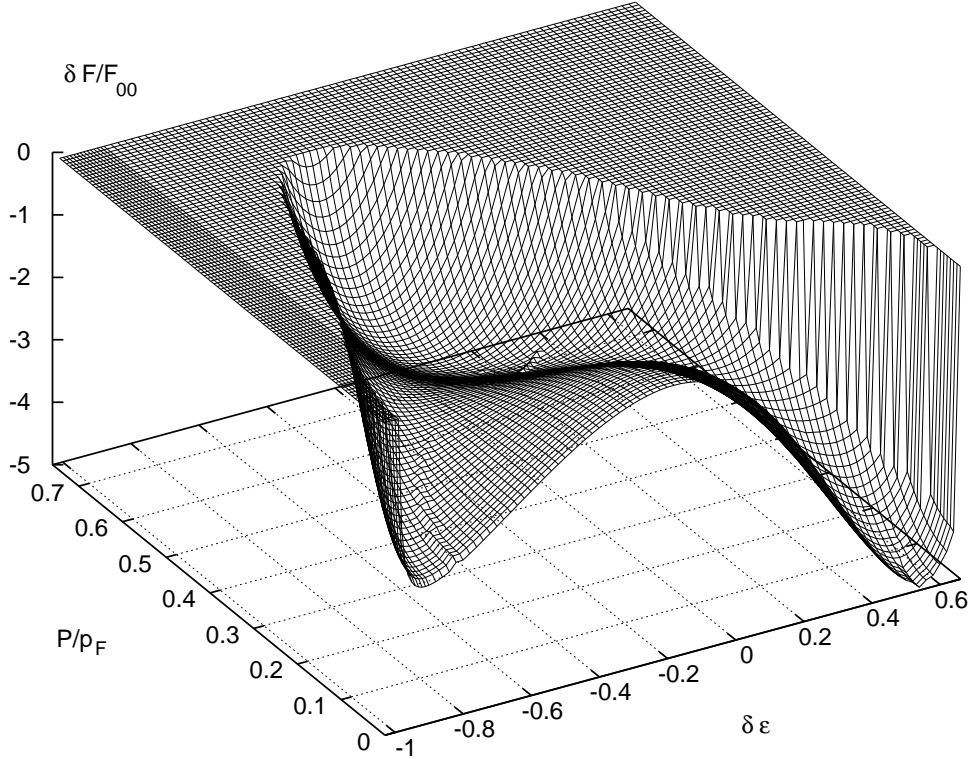


FIG. 2. The free energy difference between the superconducting and normal states  $\delta\mathcal{F}$  as a function of the Cooper pair momentum  $P$  in units of Fermi momentum and the relative deformation parameter  $\delta\epsilon$ . The free energy is normalized to its value  $\delta\mathcal{F}_{00}$  in the asymmetric BCS state. The parameters are the same as in Fig. 1.

Inversely, a negative contribution to the average chemical increases the density of states. The changes in the  $E_S$  due to the deformation do not affect qualitatively the results above. In summary of Fig. 1, the combination of the LOFF and DFS phases promotes the pairing only in the region of small  $\delta\epsilon$  and  $P$  (weak perturbation from the BCS state). For large quadrupole deformations the finite momentum is not favorable. Viewed from the LOFF phase, for large values of  $P$  the quadrupole deformations are disfavored.

Figure 2 displays the difference between the free energies of the superconducting and normal states  $\delta\mathcal{F}$  normalized to its value in the asymmetric BCS state  $\delta\mathcal{F}_{00} = \delta\mathcal{F}(P = 0, \delta\epsilon = 0)$ . The thermal contribution due to the finite-temperature entropy is numerically irrelevant for the net budget of free energies of both states. Whether the superconducting state is thermodynamically favored depends on the relative magnitude of the potential energy of the pair interactions [second term in Eq. (43)] and the difference in the kinetic energies of the normal and superconducting states. Since the energy of the pair interactions scales as the square of the pairing gap, the shape of the  $\delta\mathcal{F}$  surface closely resembles that of the pairing gap in Fig. 1. There are, however, significant quantitative differences due to the contribution from the kinetic energy of the quasiparticles. The asymmetric BCS state is the stable ground state of the system ( $\mathcal{F} < 0$ ), however its perturbations for finite  $\delta\epsilon$  and  $P$  are

unstable towards evolution to lower energy states. For the pure LOFF phase ( $\delta\epsilon = 0$ ) the ground state corresponds to finite momentum  $P \sim 0.5$  (in units of  $p_F$ ). For the pure DFS phase ( $P = 0$ ) there are two minima corresponding to  $\delta\epsilon \simeq -0.8$  and  $\delta\epsilon \simeq 0.55$ , i.e., prolate and oblate deformations of neutron Fermi spheres, respectively. In general the position of the minimum of  $\delta\mathcal{F}$  in the  $\delta\epsilon$ - $P$  plane (passing through the minima of the limiting cases) prefers either large deformations or large finite momenta. The absolute minimum energy state corresponds to  $\delta\epsilon \simeq 0.55$  and  $P = 0$ ; that is, while the LOFF phase is a local minimum state, it is generally unstable towards evolution to a pure DFS phase with oblate/prolate deformations of neutron/proton Fermi spheres. The effect of the kinetic energy contribution is to suppress the large pairing contribution for negative values of the deformation parameter. The position of the true minimum of the free energy coincides with the maximum in the pairing gap in the positive  $\delta\epsilon$  regime.

### B. LOFF phase at finite-temperature

When the system is in an isospin asymmetric state the effect of the temperature on the pairing gap and related characteristics of the superconducting state is twofold: first, at high temperatures the pairing is suppressed due to the thermal excitation of the quasiparticle states, in analogy to the classical BCS superconductors; second, at low temperatures the

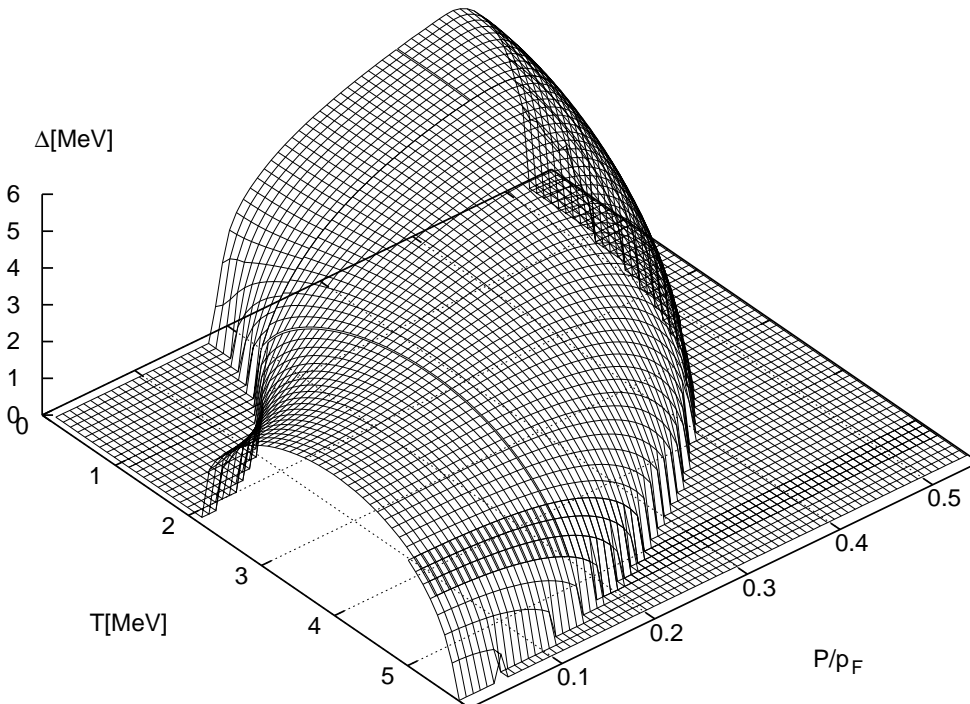


FIG. 3. The LOFF pairing gap as a function of the Cooper pair momentum and the temperature. The parameter values are the same as in Fig. 1.

pairing is enhanced by the temperature, since the thermal excitation of the quasiparticle states at different Fermi surfaces reduces the blocking effect and increases the phase-space overlap. Figure 3 shows the pairing gap in the LOFF state as a function of the temperature and finite momentum. For  $P = 0$  the asymmetric BCS state exists between two critical temperatures corresponding to the thermal stimulation and suppression of the pairing. For constant asymmetry the temperature reduces the antisymmetric part of the quasiparticle spectrum [ $E_A$  in Eq. (38)], and hence the decoherence between the quasiparticle states on different Fermi surfaces. This is responsible for the gap *reentrance* phenomenon at lower critical temperature with increasing temperature. The reduction of the contribution from the symmetric part  $E_S$  of the spectrum with increasing temperature is responsible for the quenching of the superconducting state at the upper critical temperature. At  $T = 0$ , but for finite  $P$ , analogous reentrance of the gap function is seen in Fig. 3. The existence of the lower and upper critical momenta can again be understood from the contributions of the finite momentum to the quasiparticle spectrum.

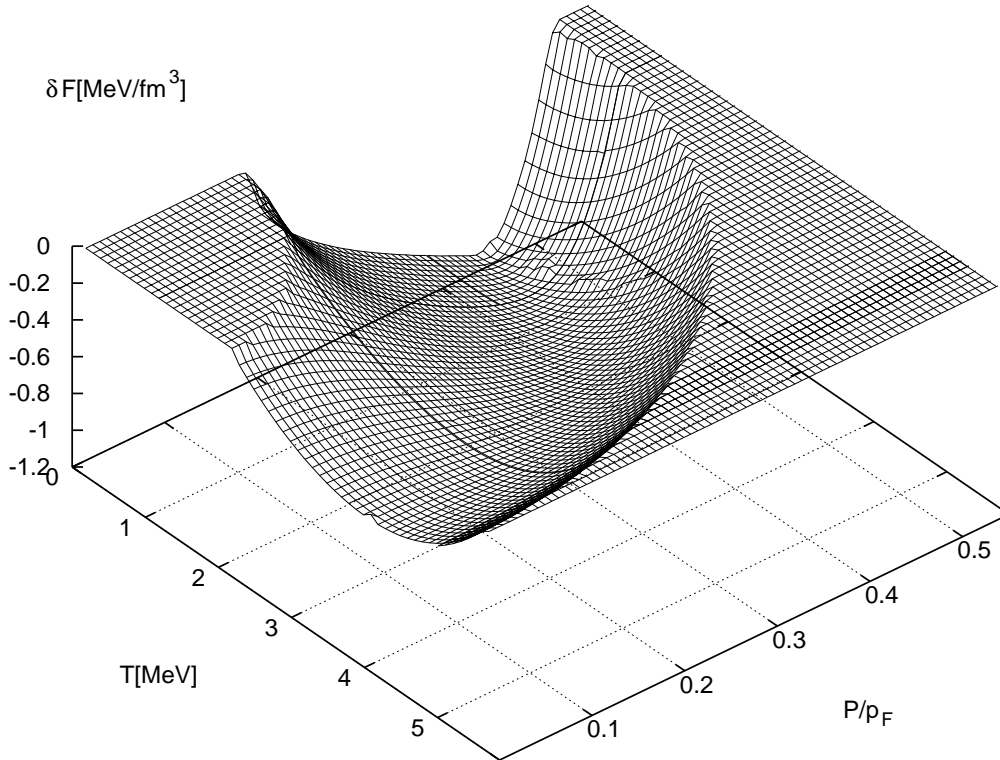


FIG. 4. The free energy difference between the superconducting and normal states  $\delta\mathcal{F}$  as a function of the Cooper pair momentum  $P$  in units of Fermi momentum and temperature. The parameters are the same as in Fig. 1.

In the general case  $P \neq 0$  and  $T \neq 0$  the reentrance phenomenon extends in the  $P - T$  plane: the pairing region of the phase diagram is bounded by the curves for the lower and upper critical values  $P_{c1}(T)$ ,  $P_{c2}(T)$ , or equivalently  $T_{c1}(P)$ ,  $T_{c2}(P)$ . The duality between the

effect of finite  $T$  on the pairing gap at fixed  $P$  to that of finite  $P$  at fixed  $T$  is evident. In Fig. 4 we show the difference between the free energies of the superconducting and normal states  $\delta\mathcal{F}$  for the LOFF phase. The true ground state here corresponds to the zero-temperature limit for pair momentum  $P/p_F \sim 0.4$ . The effect of the temperature on the LOFF phase depends on the momentum of the pair: for low momenta there is a minimum as a function of the temperature (as is also the case for the asymmetric BCS state). For large fixed momenta the temperature reduces the pairing gap. The same applies for the perturbations from the  $P = 0$  state at fixed temperature: for low temperatures the system prefers finite momenta, while for large temperatures the finite momentum only reduces the energy. The overall dependence of the free energy on the temperature and the finite momentum reflects the dependence of the pairing gap and the potential energy of the pairing interaction on these quantities.

### C. DFS phase at finite-temperature

The features seen in the phase diagram of the DFS phase at finite temperatures are analogous to those already discussed for the LOFF phase. Here we reiterate this discussion with the emphasis on the qualitative differences of these phases. The pairing gap as a function of the temperature and the relative deformation ( $\delta\epsilon$ ) is shown in Fig. 5.

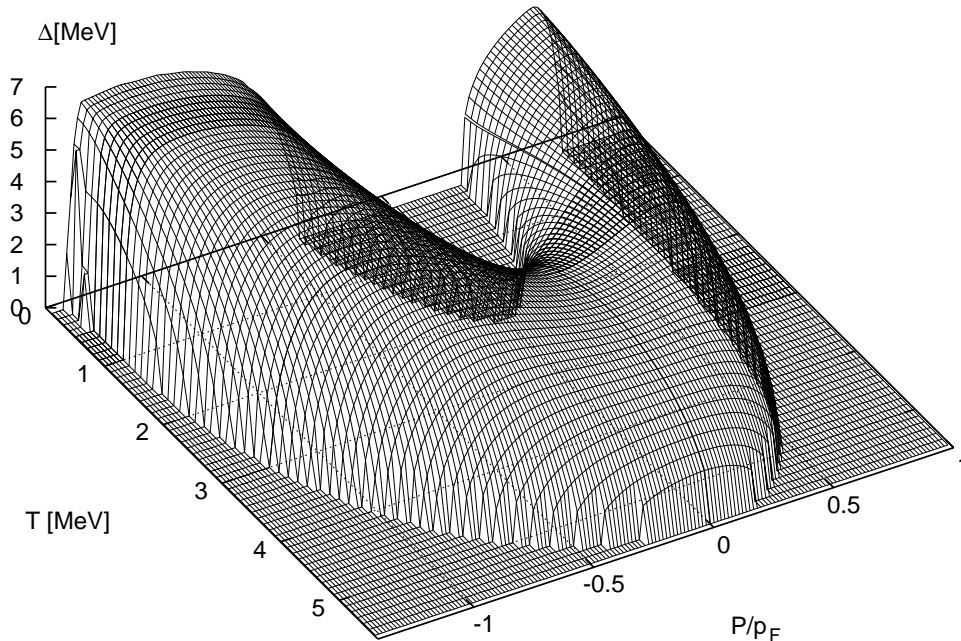


FIG. 5. The DFS pairing gap as a function of the relative deformation and the temperature. The parameter values are the same as in Fig. 1.



The reentrance effect for  $T = 0$  is seen for both signs of  $\delta\epsilon$ ; the lower critical deformation corresponds to the onset of the pairing due to the restoration of the phase-space coherence via the deformation of the spherical Fermi surface into quasiellipsoidal form. The upper critical  $\delta\epsilon$  corresponds to the loss of coherence due to the large shift in the Fermi surfaces of the paired particles. The  $T - \delta\epsilon$  duality is seen in the case where deformation vanishes (asymmetric BCS state). The lower critical temperature corresponds to the thermal stimulation of the pair correlations due to the smearing of the Fermi surfaces, while the upper critical temperature corresponds to the ordinary thermal suppression of the pairing in the BCS-normal state transition. The effect of  $\delta\epsilon$  at finite-temperatures can be understood in terms of its contribution to the antisymmetric part of the quasiparticle spectrum, in complete analogy to the LOFF phase. The reentrance effect extends in the plane  $T - \delta\epsilon$ , and the pairing region is bounded by the critical values  $\delta\epsilon_1(T)$  and  $\delta\epsilon_2(T)$ , or equivalently  $T_{c1}(\delta\epsilon)$  and  $T_{c2}(\delta\epsilon)$ . Unlike the LOFF phase these curves do not terminate at  $\delta\epsilon = 0$ , rather they show a continuous crossover from the oblate to the prolate deformation of the Fermi surface of the paired particles. For either sign of  $\delta\epsilon$  the temperature thermally stimulates the superconducting phase for small perturbations from the asymmetric BCS state corresponding to the  $\delta\epsilon = 0$  cut; for large deformations the pairing is largest in the zero-temperature limit.

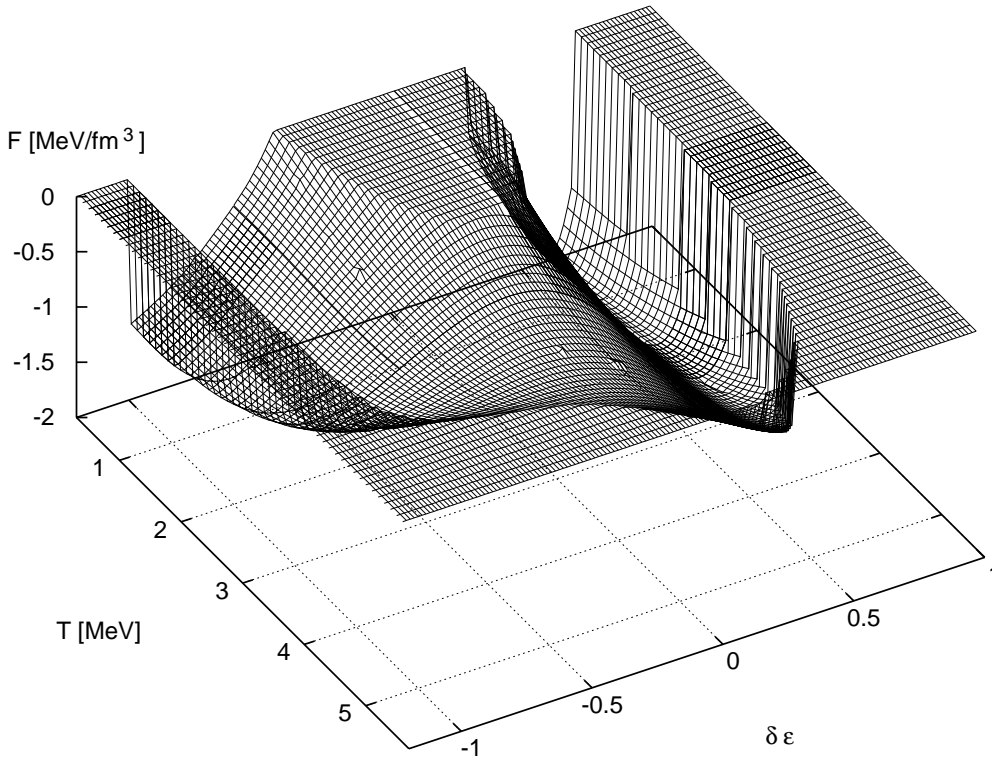


FIG. 6. The free energy difference between the superconducting and normal states  $\delta\mathcal{F}$  as a function of the relative deformation and temperature. The parameters are the same as in Fig. 1.

The effect of finite  $\delta\epsilon$  at fixed temperature is a suppression of the pairing in the high-temperature limit, while at lower temperatures there is a pronounced maximum in the pairing gap as a function of  $\delta\epsilon$ . Finally, the difference between the free energies of the superconducting and normal states  $\delta\mathcal{F}$  for the DFS phase is shown in Fig. 6. There are two minima corresponding to the oblate or prolate deformations of the Fermi surfaces of neutrons/protons. The shape of  $\delta\mathcal{F}$  is controlled by the interplay between the pairing potential energy and the kinetic energy; the contribution from the entropy difference is numerically negligible. The minima correspond to large deformations of the order 0.5 which optimize the gain in the potential energy over the loss in the kinetic energy due to the deformation; the true minimum occurs for positive  $\delta\epsilon$  at zero-temperature. While temperature stimulated pairing correlations are seen for small deviations from the BCS state, this effect is not essential, since the minimum of the  $\delta\mathcal{F}$  surface occurs at large  $\delta\epsilon$ . The DFS phase is most stable in the zero-temperature limit.

#### IV. SUMMARY AND OUTLOOK

The fermionic condensation in nuclear matter under isospin asymmetry leads to superconducting states which spontaneously break the space symmetries. We studied two realizations of such condensates - the LOFF phase, where the Cooper pairs carry finite momentum, and the DFS phase where the Fermi surfaces of the paired nucleons are deformed, to the lowest order into ellipsoidal form. A unifying feature of these phases is the deformation of the spectrum of the quasiparticle excitations at the leading (LOFF) and next-to-leading (DFS) order in the expansion in Legendre polynomials with respect to the angle between the particle momenta and the axis of symmetry breaking. When these deformations are treated simultaneously, we find that the pure DFS phase has lower energy than the LOFF phase. The combination of these phases still lower the energy of the normal system and can exist in a metastable state. In particular, the pure LOFF state could be realized in the case where the unpaired state features some intrinsic spatial asymmetries (e.g., due to the lattice in the metallic superconductors). Of course, the axis of the symmetry breaking for the LOFF and DFS phases need not be the same and, more generally, the patterns of symmetry breaking could be more complicated than those studied here (e.g., higher order multipole deformations of the Fermi surfaces).

The phase diagrams of the LOFF and DFS phases in the temperature/deformation plane show a number of unusual features: (i) two critical temperatures for the onset of the superconducting state (the reentrance phenomenon). The upper critical temperature is the analog of the BCS temperature for the superconducting-normal phase transition. The lower critical temperature is specific to asymmetric systems and results from the thermally stimulated phase-space overlap between the pairing states. (ii) There exists duality between the temperature effects and the finite-momentum or deformation effects. For example, at low temperatures the LOFF phase is characterized by two critical momenta of the Cooper pairs at which the superconducting phase sets in. (iii) The free energy of the combined LOFF and DFS phases shows local minima corresponding to negative and positive relative deformations at zero momentum of the pairs. The lowest energy corresponds to a phase with oblate neutron and prolate proton Fermi surfaces ( $\delta\epsilon$  is positive).

The realization of the  ${}^3S_1 - {}^3D_1$  pairing in bulk nuclear matter depends on a number

of factors: (i) the ratio of the pairing gap to the average chemical potential, which controls the density-temperature-dependent critical asymmetries at which the pairing vanishes; this ratio depends sensitively on the quasiparticle renormalization effects which need further study in this context. (ii) A second factor involves the asymmetries implied by the  $\beta$  equilibrium of the matter with leptons in the stellar matter; while the asymmetries derived for the normal state may serve as order of magnitude estimates, the LOFF and DFS phases under  $\beta$  equilibrium might require asymmetries largely different from those deduced for the unpaired system. (iii) The matter could prefer a state where the superconducting and normal phases coexist in a mixed phase, with superconducting “islands” immersed in the unpaired matter; the analogy to the type-I superconductors in the magnetic fields is a useful counterpart of this type of ordering. (iv) The extreme low-density asymmetric nuclear matter can support pairing in the  ${}^3S_1 - {}^3D_1$  channel at much larger asymmetries than the matter, say, at the nuclear saturation density; however, in this strong coupling regime one deals with a Bose-Einstein condensate of deuterons coexisting with a low-density neutron gas [25] and one needs an understanding of the crossover from the LOFF and DFS phases to their Bose-Einstein condensed counterparts.

We now briefly comment on possible realization of the phases with broken space symmetries in other nuclear systems. The neutron-proton pairing in finite nuclei [48–58] is an obvious candidate. The odd-number projected BCS equations contain the decoherence effects in the gap equation introduced by the extra odd particle. The resulting blocking effect is quite analogous to the phase decoherence due to the imposed neutron-proton asymmetry in the bulk nuclear matter. The problem of realization of the LOFF phase is facilitated by the fact that the pairing instability occurs for total momenta  $P \sim p_F \gg 1/R$ , where  $R$  is the radius of the nucleus. Therefore, for already medium size nuclei the influence of the surface on the condensation energy should not be large and the solutions found for the interior of the nucleus should go over to those corresponding to infinite systems. The translational symmetry is not broken by the DFS phase, therefore the finite size effects (while being generally of the same order of magnitude as for the LOFF phase) would affect the structure of the condensate to the same extent as those for the case of the pairing with undeformed Fermi surfaces.

Quite generally, the phases with broken space symmetries arise in the physical situations where the time-reversal symmetry between the paired fermion states is broken. This is the case, for example, in finite nuclei under rotation. The  ${}^1S_0$  pairing among neutrons and/or protons in such nuclei can support the LOFF or DFS like states. Similarly, the magnetic field breaks the time-reversal invariance due to the Pauli paramagnetism of neutrons and protons. The LOFF and DFS phases can arise for the case of the  ${}^1S_0$  pairing in strong magnetic fields, for example, in neutron star crusts. These phases will emerge when the interaction energy of a neutron spin with the magnetic field  $\mu_B B$ , where  $\mu_B$  is the anomalous magnetic moment of a neutron, is of the order of the pairing gap in the zero field limit. This condition is satisfied for the field strength of the order  $10^{16}$ - $10^{18}$  G (depending on the value of the pairing gap) which could occur in the highly magnetized subpopulation of neutron stars (magnetars).

As is well known, the breaking of the continuous symmetries in the infinite systems leads to collective excitations with vanishing minimal frequency (Goldstone’s theorem). The LOFF phase breaks the translational and rotational symmetries; the existence of the preferred direction in the DFS phase breaks the rotational symmetry of the system. The breaking

of continuous symmetries in the ground of these phases, therefore, implies new collective bosonic modes in asymmetric nuclear matter. In finite systems the Goldstone theorem implies collective modes which tend to zero as a certain power of the radius of the system. The observation of the Goldstone modes associated with the LOFF and/or DFS phases could provide information on the true ground state structure of the condensate under laboratory conditions, for example, in finite nuclei.

### **ACKNOWLEDGMENTS**

We would like to acknowledge the financial support by the Sonderforschungsbereich 382 of DFG.

## REFERENCES

- [1] J. W. Clark, C.-G. Källman, C.-H. Yang, and D. A. Chakkalakal, Phys. Lett. **B61**, 331 (1976).
- [2] J. A. Niskanen and J. A. Sauls (unpublished).
- [3] L. Amundsen and E. Østgaard, Nucl. Phys. **A437**, 487 (1985).
- [4] J. M. C. Chen, J. W. Clark, E. Krotschek, and R. A. Smith, Nucl. Phys. **A451**, 509 (1986).
- [5] T. L. Ainsworth, J. Wambach, and D. Pines, Phys. Lett. **B222**, 173 (1989).
- [6] M. Baldo, J. Cugnon, A. Lejeune, and U. Lombardo, Nucl. Phys. **A515**, 409 (1990).
- [7] J. Wambach, T. L. Ainsworth, and D. Pines, Nucl. Phys. **A555**, 128 (1993).
- [8] V. A. Khodel, V. V. Khodel, and J. W. Clark, Nucl. Phys. **A598**, 390 (1996).
- [9] H.-J. Schulze, J. Cugnon, A. Lejeune, M. Baldo, and U. Lombardo, Phys. Lett. **B375**, 1 (1996).
- [10] Ø. Elgarøy and M. Hjorth-Jensen, Phys. Rev. **C57**, 1174 (1998).
- [11] J. Kuckei, F. Montani, H. Müther, A. Sedrakian, nucl-th/0210010.
- [12] M. Hoffberg, A. E. Glassgold, R. W. Richardson, and M. Ruderman, Phys. Rev. Lett. **14**, 775 (1970).
- [13] T. Takatsuka and R. Tamagaki, Prog. Theor. Phys. **46**, 114 (1971).
- [14] T. Takatsuka, Prog. Theor. Phys. **48**, 1517 (1972).
- [15] R. W. Richardson, Phys. Rev. **D5**, 1883 (1972).
- [16] L. Amundsen and E. Østgaard, Nucl. Phys. **A442**, 163 (1985).
- [17] Ø. Elgarøy, L. Engvik, M. Hjorth-Jensen, and E. Osnes, Nucl. Phys. **A607**, 425 (1996).
- [18] M. Baldo, Ø. Elgarøy, L. Engvik, M. Hjorth-Jensen, and H.-J. Schulze, Phys. Rev. **C58**, 1921 (1998).
- [19] V. A. Khodel, V. V. Khodel, and J. W. Clark, Phys. Rev. Lett. **81**, 3828 (1998).
- [20] V. A. Khodel, J. W. Clark, and M. V. Zverev Phys. Rev. Lett. **87**, 031103 (2001).
- [21] V. J. Emery and A. M. Sessler, Phys. Rev. **119**, 248 (1960).
- [22] T. Alm, B. L. Friman, G. Röpke, and H. Schulz, Nucl. Phys. **A 551**, 45 (1993).
- [23] A. Sedrakian, Th. Alm, and U. Lombardo, Phys. Rev. **C55** R582 (1997)
- [24] A. Sedrakian and U. Lombardo, Phys. Rev. Lett. **84**, 602 (2000).
- [25] U. Lombardo, P. Nozieres, P. Schuck, H.-J. Schulze, and A. Sedrakian, Phys. Rev. **C64** 064314 (2001).
- [26] Ø. Elgarøy, L. Engvik, M. Hjorth-Jensen and E. Osnes, Phys. Rev. **C57**, R1069 (1998).
- [27] A. I. Akhiezer, A. A. Isayev, S. V. Peletminsky, and A. A. Yatsenko, Phys. Rev. **C63** 021304 (2001).
- [28] A. Sedrakian, G. Röpke, and T. Alm, Nucl. Phys. **A594**, 355 (1995).
- [29] T. Alm, G. Röpke, A. Sedrakian, and F. Weber, Nucl. Phys. **A604**, 491 (1996)
- [30] A. A. Abrikosov and L. P. Gor'kov, Zh. Exsp. Teor. Fiz. **39** 1781 (1960) [Sov. Phys. JETP **12**, 1243 (1961)].
- [31] A. M. Clogston, Phys. Rev. Lett. **9**, 266 (1962).
- [32] B. S. Chandrasekhar, App. Phys. Lett. **1**, 7 (1962).
- [33] L. P. Gor'kov and A. I. Rusinov, Zh. Exsp. Teor. Fiz. **46** 1363 (1964) [Sov. Phys. JETP **19**, 922 (1964)].
- [34] A. I. Larkin and Yu. N. Ovchinnikov, Zh. Exsp. Teor. Fiz. **47** 1136 (1964) [Sov. Phys. JETP **20**, 762 (1965)].

- [35] P. Fulde and R. A. Ferrell, Phys. Rev. **135**, 550 (1964).
- [36] A. Sedrakian, Phys. Rev. **C63** 025801 (2001).
- [37] A. A. Isayev, Phys. Rev. **C65** 031302 (2002).
- [38] M. G. Alford, Ann. Rev. Nucl. Part. Sci. **51**, 131 (2001).
- [39] K. Rajagopal, AIP Conf. Proc. **602**, 339 (2001) [Nucl. Phys. A **702**, 25 (2002)].
- [40] K. Rajagopal and F. Wilczek, in *Frontier of Particle Physics / Handbook of QCD*, edited by M. Shifman (World Scientific Singapore, 2002), chap. 35.
- [41] M. Alford, J. A. Bowers, and K. Rajagopal, Phys. Rev. D **63**, 074016 (2001).
- [42] A. K. Leibovich, K. Rajagopal, and E. Shuster, Phys. Rev. D **64**, 094005 (2001).
- [43] J. A. Bowers, J. Kundu, K. Rajagopal, and E. Shuster, Phys. Rev. D **64**, 014024 (2001).
- [44] R. Casalbuoni, R. Gatto, M. Mannarelli, and G. Nardulli, Phys. Rev. D **66**, 014006 (2002).
- [45] J. Bowers and K. Rajagopal, arXiv:hep-ph/0204079.
- [46] H. Mütter and A. Sedrakian, Phys. Rev. Lett. **88**, 252503 (2002).
- [47] L. Kadanoff and G. Baym, *Quantum Statistical Mechanics* (Benjamin, New York, 1962).
- [48] P. Ring and P. Schuck, *The Nuclear Many-Body Problem* (Springer-Verlag, New York, 1980).
- [49] A. L. Goodman, Adv. Nucl. Phys. **11**, 263 (1979).
- [50] H. H. Wolter, A. Faessler, and P. U. Sauer, Nucl. Phys. **A 167**, 108, (1971).
- [51] A. L. Goodman, Phys. Rev. **C60**, 014311 (1999).
- [52] J. Engel, K. Langanke, and P. Vogel, Phys. Lett. B **389**, 211 (1996).
- [53] J. Engel, S. Pittel, M. Stoitsov, P. Vogel, and J. Dukelsky, Phys. Rev. **C55**, 1781 (1997).
- [54] J. Dobaczewski, W. Nazarewicz, T. R. Werner, J. F. Berger, C. R. Chinn, and J. Decharge, Phys. Rev. **C53**, 2809 (1996).
- [55] W. Satula and R. Wyss, Phys. Lett. B **393**, 1 (1997).
- [56] O. Civitarese, M. Reboiro, and P. Vogel, Phys. Rev. **C56**, 1840 (1997).
- [57] O. Civitarese and M. Reboiro, Phys. Rev. **C56**, 1179 (1997).
- [58] G. Röpke, A. Schnell, P. Schuck, and U. Lombardo, Phys. Rev. C **61**, 024306 (2000).